

Gluonic Effects on $g - 2$: Holographic View

Masafumi Kurachi,^{1,*} Shinya Matsuzaki,^{2,3,†} and Koichi Yamawaki^{1,‡}

¹ *Kobayashi-Maskawa Institute for the Origin of Particles and the Universe (KMI)
Nagoya University, Nagoya 464-8602, Japan.*

² *Institute for Advanced Research, Nagoya University, Nagoya 464-8602, Japan.*

³ *Department of Physics, Nagoya University, Nagoya 464-8602, Japan.*

We study “gluonic effects” (gluon condensation effects) on the hadronic leading order (HLO) contributions to the anomalous magnetic moment ($g-2$) of leptons, based on a holographic model having explicit gluonic mode introduced for consistency with the operator product expansion of QCD. We find gluonic enhancement of HLO contributions to the muon $g - 2$ by about 6%, which nicely fills in the gap between the holographic estimate without gluonic effects and the phenomenological one using the experimental data as inputs. Similar calculations including the gluonic effects for the electron and the tau lepton $g - 2$ are also carried out in good agreement with the phenomenological estimates. We then apply our holographic estimate to the Walking Technicolor (WTC) where large techni-gluonic effects were shown to be vital for the Technidilaton, (pseudo) Nambu-Goldstone boson of the (approximate) scale symmetry of WTC, to be naturally as light as 125 GeV. It is shown that the value of the techni-HLO contributions to the muon $g - 2$ is 10-100 times enhanced by inclusion of the same amount of the gluonic effects as that realizing the 125 GeV Technidilaton, although such an enhanced techni-HLO contribution is still negligibly small compared with the current deviation of the Standard Model prediction of the muon $g - 2$ from the experiments. The techni-HLO contributions to the tau lepton $g - 2$ is also discussed, suggesting a possible phenomenological relevance to be tested by the future experiments.

I. INTRODUCTION

Holography, based on AdS/CFT (anti-de-Sitter space/conformal field theory) correspondence [1], has been extensively used to analyze strongly coupled gauge systems. For instance, QCD can be reformulated based on the gauge-gravity duality, either in the bottom-up approach [2, 3] modeled as a five-dimensional gauge theory defined in an AdS background, or in the top-down approach [4] starting with a stringy setting. Such models of holographic QCD have succeeded well in reproducing several important properties for QCD hadrons within a theoretically expected size of uncertainties. In particular, the bottom-up approach can be made to reproduce the QCD in the all energy region, from the high energy behavior through the operator product expansion (OPE) down to the low energy resonance physics: The correct power behaviors in OPE for the chiral condensate and the gluon condensate are realized by introduction of the bulk (chiral non-singlet) scalar field, Φ_S , corresponding to the $\bar{q}q$ operator and (chiral singlet) bulk gluonic field, Φ_G , respectively [5], which is contrasted to the top-down approach having high energy behavior completely different than that of QCD. The bottom-up holography so constructed can provide us with novel insights into the strong dynamics through the highly nontrivial effects of the gluonic dynamics: It reproduces nicely the known value of the gluon condensate which is otherwise zero, and the mass of a_1 meson of the right magnitude.

Such a bottom-up holographic QCD model having gluon condensation effects (hereafter, we will use the phrase “gluonic effects” to refer to the gluon condensation effects) Φ_G was further applied [5] to the Walking Technicolor (WTC) model [7] which has an approximate scale symmetry and a large anomalous dimension $\gamma_m = 1$, and further predicts a light composite Higgs dubbed “Technidilaton (TD)” as a pseudo Nambu-Goldstone boson of the approximate scale symmetry. The holographic WTC of Ref. [5] was formulated through a simple replacement of $\gamma_m = 0$ for QCD by $\gamma_m = 1$ in the mass parameter of the bulk scalar Φ_S in the holographic QCD with Φ_G , which was found [6] to have more intriguing gluonic effects than in those of the holographic QCD: Large gluonic effects due to Φ_G in WTC actually realize an idealized limit where TD [7, 8] as a flavor-singlet scalar fermionic bound state (lowest Kaluza-

*kurachi@kmi.nagoya-u.ac.jp

†synya@hken.phys.nagoya-u.ac.jp

‡yamawaki@kmi.nagoya-u.ac.jp

Klein (KK) mode of Φ_S ^{#1} has a vanishingly small mass compared with the typical symmetry breaking scale $4\pi F_\pi$ (F_π : techni-pion decay constant), and hence it can naturally be as light as 125 GeV to be identified as the Higgs boson discovered at the LHC [9]. This is in sharp contrast to the earlier nonperturbative studies based on the ladder approximation [10, 11] without nonperturbative gluonic dynamics, which yields a substantially smaller scalar mass than in the QCD case, though it does not have such an idealized massless limit and hence no natural framework for the light TD^{#2}. Therefore, proper inclusion of gluonic effects is important not only for the study of QCD, but also, or more significantly, for the realistic WTC calculations.

Holographic computations are generically done through evaluating Green functions constructed from (techni-)quark and gluon currents, so that the main outputs are made from the current correlators, including full information on masses and couplings for the associated mesons and glueball coupled to those currents. Once the vector current correlator is obtained from the holographic calculation, it is possible to translate it into the electromagnetic current correlator, $\Pi_{\text{em}}(Q^2)$, from which we can estimate the (techni-)hadronic leading order (HLO) contribution to the anomalous magnetic moment of the muon (the muon $g-2$). Actually, in Ref. [14] a holographic estimation of such a QCD HLO contribution was done based on an earlier bottom-up holographic model [3], in which, however, effects from the gluon condensation are not incorporated.

In this paper, we study the gluonic effects on the muon $g-2$ in QCD and WTC through the (techni-)HLO contribution, based on a recently published holographic model in the bottom-up approach [5, 6]. The model has 3 holographic parameters (z_m, ξ, G) to be explained later; ξ and G , roughly corresponding to the chiral condensate and the gluon condensate, respectively, at the infrared brane located at z_m . By fixing the values $f_\pi = 92.4$ MeV and $M_\rho = 775.49$ MeV as inputs, we have ξ and z_m as functions of G . Accordingly, we show all other hadronic observables given as functions of a single holographic gluonic parameter G : While the mass of the flavor-singlet scalar $f_0(1370)$ and the scalar glueball are insensitive to the value of G , the mass of a_1 meson and the gluon condensate which are fairly sensitive to G so that we can determine the value of $G \simeq 0.25$ nicely fitting the reality of all the observables studied [5, 6].

We then estimate the HLO contributions including the gluon-condensation effect, based on a formula for the HLO directly evaluated by the current correlator in the (theoretically more tractable) *space-like momentum* in contrast to the conventional one converting it to the dispersion integral from the time-like contributions where the experimental data are available. The results show that the proper inclusion of gluon-condensation effect $G \simeq 0.25$ causes about 6% enhancement of the HLO contribution to the muon $g-2$: $a_\mu^{\text{HLO}}|_{N_f=2} \simeq 505 \times 10^{-10}$, $a_\mu^{\text{HLO}}|_{N_f=3} \simeq 606 \times 10^{-10}$, which are compared to the previous calculation [14] without gluon-condensation effect $G = 0$: $a_\mu^{\text{HLO}}|_{N_f=2} \simeq 476 \times 10^{-10}$, $a_\mu^{\text{HLO}}|_{N_f=3} \simeq 571 \times 10^{-10}$, respectively. This enhancement makes the prediction of holographic calculation of the HLO contribution very close to the known value [15] from the phenomenological estimate using the experimental inputs $a_\mu^{\text{HLO}}|_{\pi+\pi^-} = (504.2 \pm 3.0) \times 10^{-10}$ and $a_\mu^{\text{HLO}}|_{\text{full}} = (694.9 \pm 4.3) \times 10^{-10}$, respectively. We also calculate the HLO contributions to the electron and the tau lepton $g-2$, and show that the holographic predictions are quite consistent with the known values as well.

Considering the fact that the energy scales important for determining the HLO effects are hierarchically different depending on the lepton species, it is remarkable that the holographic calculations, with proper inclusion of gluon-condensation effect, can reproduce HLO contributions to $g-2$ for all the leptons. This means that with inclusion of the gluonic contributions the holographic calculation of $\Pi_{\text{em}}(Q^2)$ is quite reliable in a *wide range of energy scale*, and remarkably in the (theoretically tractable) continuous space-like momentum, not just in the range of the (discrete) time-like momentum where the resonance parameters are fitted in the conventional holographic studies in the zero-width approximation (large N_c limit).

Encouraged by this success, we apply the same holographic calculations of the HLO-type contributions to the $g-2$ from the WTC, with $\gamma_m = 0$ in QCD simply replaced by $\gamma_m = 1$ through the bulk scalar mass. We first show the gluonic effects on various observables in WTC, including the mass of the flavor-singlet scalar meson M_ϕ identified with TD, which can be as light as the 125 GeV boson discovered at the LHC for a large gluonic effect with $G \simeq 10$ [6]. Then we study the effect of such a large G on the muon $g-2$ through the techni-HLO contribution, which we find as large as 100 times of the value for $G = 0$: Imposing a typical constraint on the Peskin-Takeuchi S parameter [16] from

^{#1} Note that a scalar techni-glueball as the lowest KK mode of Φ_G has no direct relevance to the electroweak symmetry breaking, since the technigluons carry no electroweak charge, and hence cannot be identified with the TD, or composite Higgs, whose constituents must carry the electroweak charge.

^{#2} We actually have a formal limit of massless TD through the ladder estimate for the Partially Conserved Dilatation Current (PCDC) relation, which involves mass M_ϕ and the decay constant F_ϕ of the TD ϕ only in the form of a product, $M_\phi F_\phi = \mathcal{O}(F_\pi^2)$, (not separately). This implies that a massless TD limit $M_\phi/F_\pi \rightarrow 0$ is formally realized only when $F_\phi/F_\pi \rightarrow \infty$, or the coupling vanishes (decoupled dilaton) [5, 12]. Nevertheless, it so happened that the mass estimated by the ladder PCDC actually can be parametrically tuned to be 125 GeV in such a way as to be consistent with the current LHC data, being still far from the decoupling limit [13].

the electroweak (EW) precision test, $S = 0.1$, the enhancement is about 10 times and by relaxing the constraint on S parameter as $0.1 < S < 1.0$ for the reason described in the text, the techni-HLO contribution can be further enhanced by another factor of about 10. For all such enhancements, however, we show that the techni-HLO contributions from WTC dynamics is negligibly small compared to the HLO contributions from QCD. It is then very unlikely that the contributions from WTC dynamics can explain the inconsistency by about 3.3σ between the experimental value of the muon $g - 2$ and the Standard Model (SM) prediction of it. We also mention the techni-HLO contribution to the tau $g - 2$, which may become relevant in future experiments.

The paper is organized as follows: In the next section, we review the model [5] and formulas which are needed for the calculations of various physical quantities studied in this paper. In section III, we study the gluonic effect of the muon $g - 2$ through the holographic QCD calculation of HLO contribution, based on the successful inclusion of the gluonic effects on the various hadronic observables in Ref. [5]. In section IV, we use similar holographic calculations for the study of WTC effects on the $g - 2$. Section V is devoted to discussions and summary of the paper.

II. HOLOGRAPHIC MODEL AND FORMULAS

The model [5] we shall employ is based on deformations of a bottom-up approach for successful holographic dual of QCD [2, 3]. The model is described as $SU(N_f)_L \times SU(N_f)_R$ gauge theory defined on the five-dimensional AdS space-time, which is characterized by the metric $ds^2 = g_{MN}dx^M dx^N = (L/z)^2 (\eta_{\mu\nu} dx^\mu dx^\nu - dz^2)$ with $\eta_{\mu\nu} = \text{diag}[1, -1, -1, -1]$. Here, M and N (μ and ν) represent five-dimensional (four-dimensional) Lorentz indices, and L denotes the curvature radius of the AdS background. The fifth direction, denoted as z , is compactified on an interval extended from the ultraviolet (UV) brane located at $z = \epsilon$ to the infrared (IR) brane at $z = z_m$, i.e., $\epsilon \leq z \leq z_m$. The UV cutoff ϵ will be taken to be 0 after all calculations are done. In addition to the bulk left- (L_M) and right- (R_M) gauge fields, we introduce a bulk scalar Φ_S which transforms as a bifundamental representation field under the $SU(N_f)_L \times SU(N_f)_R$ gauge symmetry, and therefore it is considered to be dual to the quark bilinear operator $\bar{q}q$. The mass-parameter m_{Φ_S} is then related to γ_m as

$$m_{\Phi_S}^2 = -\frac{(3 - \gamma_m)(1 + \gamma_m)}{L^2}. \quad (1)$$

We take $\gamma_m = 0$ when we apply this holographic model to the study of the actual QCD, while we take $\gamma_m = 1$ when we consider the model as a dual of WTC. The action of the model is given as [5]

$$S_5 = S_{\text{bulk}} + S_{\text{UV}} + S_{\text{IR}}, \quad (2)$$

where S_{bulk} denotes the five-dimensional bulk action,

$$\begin{aligned} S_{\text{bulk}} = & \int d^4x \int_{\epsilon}^{z_m} dz \sqrt{g} \frac{1}{g_5^2} e^{c_G g_5^2 \Phi_G} \left[\frac{1}{2} \partial_M \Phi_G \partial^M \Phi_G \right. \\ & + \text{Tr}[D_M \Phi_S^\dagger D^M \Phi_S - m_{\Phi_S}^2 \Phi_S^\dagger \Phi_S] \\ & \left. - \frac{1}{4} \text{Tr}[L_{MN} L^{MN} + R_{MN} R^{MN}] \right], \quad (3) \end{aligned}$$

and $S_{\text{UV,IR}}$ the boundary actions which are given in Ref. [6]. The covariant derivative acting on Φ_S in Eq.(3) is defined as $D_M \Phi_S = \partial_M \Phi_S + i L_M \Phi_S - i \Phi_S R_M$, where $L_M (R_M) \equiv L_M^a (R_M^a) T^a$ with T^a being the generators of $SU(N_f)$ which are normalized as $\text{Tr}[T^a T^b] = \delta^{ab}$. $L(R)_{MN}$ is the five-dimensional field strength which is defined as $L(R)_{MN} = \partial_M L(R)_N - \partial_N L(R)_M - i[L(R)_M, L(R)_N]$, and g is defined as $g = \det[g_{MN}] = (L/z)^{10}$. A salient feature of the model is the extra bulk scalar Φ_G introduced in Eq.(3) in order to reproduce the correct asymptotic behavior of the QCD. This is a bulk field which is dual to the gluon condensate $\langle \alpha_s G_{\mu\nu}^2 \rangle$ in QCD. Here, α_s is related to the QCD gauge coupling g_s by $\alpha_s = g_s^2/(4\pi)$. Since $\langle \alpha_s G_{\mu\nu}^2 \rangle$ is a singlet under the chiral $SU(N_f)_L \times SU(N_f)_R$ symmetry, the dual-bulk scalar Φ_G has to be a real field. We take $\dim(\alpha_s G_{\mu\nu}^2) = 4$, thus the corresponding bulk-mass parameter becomes $m_{\Phi_G}^2 = 0$. The gauge coupling g_5 and a parameter c_G appearing in the action are fixed as

$$\frac{L}{g_5^2} = \frac{N_c}{12\pi^2}, \quad c_G = -\frac{L}{16\pi g_5^2} = -\frac{N_c}{192\pi^3}, \quad (4)$$

so that the model reproduces the OPE in QCD (see later discussions) [5].

We shall begin with the bulk scalar sector in Eq.(3). The bulk scalar fields Φ_S and Φ_G are parametrized as

$$\Phi_S(x, z) = \frac{1}{\sqrt{2}} \left(v_S(z) + \frac{\sigma_S(x, z)}{\sqrt{N_f}} \right) e^{2i\pi(x, z)/v_S(z)}, \quad (5)$$

$$\chi_G(x, z) \equiv e^{c_G g_5^2 \Phi_G/2} = v_{\chi_G}(z) e^{\sigma_{\chi_G}(x, z)/v_{\chi_G}(z)}, \quad (6)$$

with the vacuum expectation values (VEVs), $v_S = \sqrt{2}\langle\Phi_S\rangle$ and $v_{\chi_G} = \langle\chi_G\rangle$. We hereafter disregard (techni-)pion fields π which will not be relevant for the present study. The boundary conditions for $v_S(z)$ are [5, 6, 17]:

$$v_S(\epsilon) = \begin{cases} \left(\frac{\epsilon}{L}\right) c_S^{\gamma_m=0} M & \text{for } \gamma_m = 0 \\ \left(\frac{\epsilon}{L}\right)^2 \log \frac{z_m}{\epsilon^2} c_S^{\gamma_m=1} M & \text{for } \gamma_m = 1 \end{cases}, \quad (7)$$

$$v_S(z_m) = \frac{\xi}{L}, \quad (8)$$

where M stands for the current mass of (techni-)quarks, and the IR value ξ is related to the (techni-)quark condensate $\langle\bar{q}q\rangle$. The parameter $c_S^{\gamma_m}$ has been introduced which can arise from the ambiguity of the definition for the current mass M , and is fixed to be $c_S^{\gamma_m=0} = \sqrt{3}$ for QCD and $c_S^{\gamma_m=1} = \sqrt{3}/2$ for WTC, by matching the UV asymptotic form of the scalar current correlator to the form predicted from the operator product expansion [6].

The boundary conditions for $v_{\chi_G}(z)$ are taken for both QCD and WTC cases as

$$v_{\chi_G}(\epsilon) = e^{\frac{c_G}{2} \frac{g_5^2}{L} M'} = e^{-\frac{1}{32\pi} L M'}, \quad (9)$$

$$v_{\chi_G}(z_m) = 1 + G, \quad (10)$$

where M' becomes an external source for the (techni-)gluon condensate operator $(\alpha_s G_{\mu\nu}^2)$, and G is a parameter which is associated with the (techni-)gluon condensate $\langle\alpha_s G_{\mu\nu}^2\rangle$. The solutions of the VEVs $v_S(z)$ and $v_{\chi_G}(z)$ in the limit where $M \rightarrow 0$ and $M' \rightarrow 0$ are given as [5]

$$v_S(z) = \begin{cases} \frac{\xi(1+G)}{L} \frac{(z/z_m)^3}{1+G(z/z_m)^4} & \text{for } \gamma_m = 0 \\ \frac{\xi(1+G)}{L} \frac{(z/z_m)^2}{1+G(z/z_m)^4} \frac{\log(z/\epsilon)}{\log(z_m/\epsilon)} & \text{for } \gamma_m = 1 \end{cases} \quad (11)$$

$$v_{\chi_G}(z) = 1 + G \left(\frac{z}{z_m} \right)^4. \quad (12)$$

One can solve the equations of motion for the bulk scalars σ_S and σ_{χ_G} with the UV boundary conditions similar to those in Eqs. (7) and (9) with M and M' replaced by sources $(s(x), g(x))$ for the scalar and gluonic currents $(J_S(x), J_G(x))$. Putting their solutions back into the action S_5 in Eq.(2), one can then obtain the generating functional $W[s(x), g(x)]$ holographically dual to QCD or WTC. The chiral condensate and gluon condensate ($\langle\bar{q}q\rangle$ and $\langle\alpha_s G_{\mu\nu}^2\rangle$) are thus calculated by performing $\delta W/\delta s(x)$ and $\delta W/\delta g(x)$, respectively:

$$\langle\bar{q}q\rangle_{1/z_m} = -\frac{c_S^{\gamma_m}(3-\gamma_m)N_c \xi(1+G)}{12\pi^2 z_m^3}, \quad c_S^{\gamma_m} = \begin{cases} \sqrt{3} & \text{for } \gamma_m = 0 \\ \sqrt{3}/2 & \text{for } \gamma_m = 1 \end{cases}, \quad (13)$$

$$\langle\alpha_s G_{\mu\nu}^2\rangle = \frac{32N_c G}{3\pi z_m^4}, \quad (14)$$

where $\langle\bar{q}q\rangle_{1/z_m}$ is the chiral condensate renormalized at $\mu = 1/z_m$ [17]. The chiral condensate renormalized at generic scale μ is given by $\langle\bar{q}q\rangle_\mu = Z_m^{-1}(\mu z_m) \cdot \langle\bar{q}q\rangle_{1/z_m}$ with $Z_m^{-1}(\mu z_m) = (\mu z_m)^{\gamma_m}$. One can also calculate the scalar meson (TD) mass M_S and glueball mass M_G by evaluating the lowest poles of the scalar and gluonic current correlators [6] to find the following eigenvalue equations:

$$M_S : \frac{3}{2}\xi^2 J_{1-\gamma_m}(M_S z_m) = (M_S z_m) J_{2-\gamma_m}(M_S z_m), \quad (15)$$

$$M_G : J_1(M_G z_m) = 0, \quad (16)$$

where J is the Bessel function of the first kind.

We shall move on to the gauge sector in Eq.(3). We define the five-dimensional vector and axial-vector gauge fields V_M and A_M as

$$V_M = \frac{L_M + R_M}{\sqrt{2}}, \quad A_M = \frac{L_M - R_M}{\sqrt{2}}. \quad (17)$$

It is convenient to work with the gauge-fixing $V_z = A_z \equiv 0$ and take the boundary conditions $V_\mu(x, \epsilon) = v_\mu(x)$, $A_\mu(x, \epsilon) = a_\mu(x)$ and $\partial_z V_\mu(x, z)|_{z=z_m} = \partial_z A_\mu(x, z)|_{z=z_m} = 0$, where $v_\mu(x)$ and $a_\mu(x)$ correspond to sources for the vector and axial-vector currents, respectively. We then solve the equations of motion for (the transversely polarized components of) $V_\mu(x, z)$ and $A_\mu(x, z)$ and substitute the solutions back into the action in Eq.(3), to obtain the generating functional $W[v_\mu, a_\mu]$ holographically dual to QCD or WTC. Then the vector and the axial-vector current correlators are obtained in a way similar to the case of the scalar sector. The correlators are defined as

$$i \int d^4x e^{iqx} \langle 0 | T J_V^{a\mu}(x) J_V^{b\nu}(0) | 0 \rangle = \delta^{ab} \left(\frac{q^\mu q^\nu}{q^2} - \eta^{\mu\nu} \right) \Pi_V(-q^2), \quad (18)$$

$$i \int d^4x e^{iqx} \langle 0 | T J_A^{a\mu}(x) J_A^{b\nu}(0) | 0 \rangle = \delta^{ab} \left(\frac{q^\mu q^\nu}{q^2} - \eta^{\mu\nu} \right) \Pi_A(-q^2), \quad (19)$$

where the currents are defined as

$$J_V^{a\mu} = \bar{\psi} \left(\frac{T^a}{\sqrt{2}} \right) \gamma^\mu \psi, \quad (20)$$

$$J_A^{a\mu} = \bar{\psi} \left(\frac{T^a}{\sqrt{2}} \right) \gamma^\mu \gamma_5 \psi. \quad (21)$$

$\Pi_V(Q^2)$ and $\Pi_A(Q^2)$ (where $Q \equiv \sqrt{-q^2}$ is the Euclidean momentum) are expressed as

$$\Pi_V(Q^2) = \frac{N_c}{12\pi^2} \frac{\partial_z V(Q^2, z)}{z} \Bigg|_{z=\epsilon \rightarrow 0}, \quad (22)$$

$$\Pi_A(Q^2) = \frac{N_c}{12\pi^2} \frac{\partial_z A(Q^2, z)}{z} \Bigg|_{z=\epsilon \rightarrow 0}, \quad (23)$$

where the vector and axial-vector profile functions $V(Q^2, z)$ and $A(Q^2, z)$ are defined as $V_\mu(q, z) = v_\mu(q)V(Q^2, z)$ and $A_\mu(q, z) = a_\mu(q)A(Q^2, z)$ with the Fourier transforms of $v_\mu(x)$ and $a_\mu(x)$. These profile functions satisfy the following equations:

$$[-Q^2 + \omega^{-1}(z)\partial_z \omega(z)\partial_z] V(Q^2, z) = 0, \quad (24)$$

$$\left[-Q^2 + \omega^{-1}(z)\partial_z \omega(z)\partial_z - 2 \left(\frac{L}{z} \right)^2 [v_S(z)]^2 \right] A(Q^2, z) = 0, \quad (25)$$

$$\omega(z) \equiv \frac{L}{z} \left(1 + G \left(\frac{z}{z_m} \right)^4 \right)^2, \quad (26)$$

with the boundary conditions $V(Q^2, z)|_{z=\epsilon \rightarrow 0} = A(Q^2, z)|_{z=\epsilon \rightarrow 0} = 1$ and $\partial_z V(Q^2, z)|_{z=z_m} = \partial_z A(Q^2, z)|_{z=z_m} = 0$. It is worth mentioning that both the vector and the axial-vector current correlators involve gluonic effects through G . Most notably, we have

$$\Pi_V(Q^2) \Bigg|_{(1/z_m)^2 \ll Q^2 < (1/\epsilon)^2} = Q^2 \left[\frac{L}{2g_5^2} \log Q^2 + c_G \frac{2g_5^2}{3L} \frac{\langle \alpha_s G_{\mu\nu}^2 \rangle}{Q^4} + \dots \right], \quad (27)$$

in accord with the OPE in QCD:

$$\Pi_V^{(\text{QCD})}(Q^2) \Bigg|_{\text{OPE}} = Q^2 \left[\frac{N_c}{24\pi^2} \log \left(\frac{Q^2}{\mu^2} \right) - \frac{1}{24\pi} \frac{\langle \alpha_s G_{\mu\nu}^2 \rangle}{Q^4} + \dots \right], \quad (28)$$

which was the basis for the parameter matching in Eq.(4). Were it not for the Φ_G term, we would not reproduce the correct gluon condensate term $1/Q^4$ in the QCD asymptotics and also in WTC. Therefore the physical quantities which are related to these correlators, including the muon $g-2$, are influenced by the existence of gluonic dynamics.

The vector and axial-vector current correlators, Π_V and Π_A , can be expanded in terms of towers of the vector and axial-vector resonances. We then identify the lowest poles for $\Pi_{V,A}$ as the (techni-) ρ and a_1 mesons. Their masses, M_ρ and M_{a_1} , are calculated by solving the eigenvalue equations for the vector and axial-vector profile functions [5]:

$$[M_\rho^2 + \omega^{-1}(z)\partial_z\omega(z)\partial_z] V(z) = 0, \quad (29)$$

$$\left[M_{a_1}^2 + \omega^{-1}(z)\partial_z\omega(z)\partial_z - 2\left(\frac{L}{z}\right)^2 [v_S(z)]^2 \right] A(z) = 0, \quad (30)$$

with the same boundary conditions $V(\epsilon) = A(\epsilon) = 0$ and $\partial_z V(z)|_{z=z_m} = \partial_z A(z)|_{z=z_m} = 0$. We thus find M_ρ and M_{a_1} as functions of the model parameters ξ , G and γ_m with the overall scale set by z_m : $M_\rho = z_m^{-1} \cdot \widetilde{M}_\rho(G)$ and $M_{a_1} = z_m^{-1} \cdot \widetilde{M}_{a_1}(\xi, G, \gamma_m)$.

The (techni-)pion decay constant is expressed as $f_\pi^2 = \Pi_V(0) - \Pi_A(0)$, which is, in the case of WTC, related to the EW scale $v_{EW} \simeq 246$ GeV as $F_\pi = v_{EW}/\sqrt{N_D}$. Here, N_D denotes the number of EW doublets, which is fixed to be 1 in the case of QCD. The present model enables us to express f_π as a function of ξ , G , γ_m and z_m [5]:

$$f_\pi^2 = \frac{N_c}{12\pi^2} \frac{\widetilde{F}^2(\xi, G, \gamma_m)}{z_m^2}, \quad (31)$$

where $\widetilde{F}^2 = -\partial_t A(Q^2 = 0, t = z/z_m)/t|_{t=\epsilon/z_m \rightarrow 0}$.

The S parameter [16] is calculated from Π_V and Π_A as $S = -16\pi L_{10} = -4\pi N_D [\Pi'_V(0) - \Pi'_A(0)]$, where $\Pi'_{V,A}(0) \equiv d\Pi_{V,A}(Q^2)/dQ^2|_{Q^2=0}$. Thus S is expressed as a function of two parameters ξ and G [5] once γ_m is fixed:

$$S = -16\pi L_{10} = \frac{N_D N_c}{3\pi} \int_{t_\epsilon}^1 \frac{dt}{t} v_\chi^2(t) (1 - [A(Q^2 = 0, t = z/z_m)]^2), \quad (32)$$

where $t_\epsilon = \epsilon/z_m (\rightarrow 0)$.

Once $\Pi_V(Q^2)$ is calculated in the holographic model, the electromagnetic current correlator $\Pi_{em}(Q^2)$ is obtained as

$$\Pi_{em}(Q^2) = 2 \left(\sum_f q_f^2 \right) \frac{\Pi_V(Q^2)}{Q^2}, \quad (33)$$

where the summation runs over all the fermion flavors f with their electromagnetic charge denoted as q_f . Here, we defined electromagnetic current correlator as

$$i \int d^4x e^{iqx} \langle 0 | T J_{em}^\mu(x) J_{em}^\nu(0) | 0 \rangle = (q^2 \eta^{\mu\nu} - q^\mu q^\nu) \Pi_{em}(-q^2), \quad (34)$$

where the electromagnetic current is defined as $J_{em}^\mu = \sum_f q_f \bar{\psi}_f \gamma^\mu \psi_f$. With the electromagnetic current correlator given, the (techni-)hadronic leading order (HLO) contribution to the muon $g-2$ is calculated to be [18] (For a graphical expression, see Fig. 1.)

$$\left. \left(\frac{g-2}{2} \right) \right|_{(\text{techni})\text{HLO}} \equiv a_\mu^{(\text{techni})\text{HLO}} = 4\pi^2 \left(\frac{\alpha_{em}}{\pi} \right)^2 \int_0^\infty dQ^2 f(Q^2) \Pi_{em}^R(Q^2), \quad (35)$$

where $\alpha_{em} = e^2/(4\pi)$ with e being the electromagnetic coupling constant. $\Pi_{em}^R(Q^2)$ is the renormalized electromagnetic current correlator defined as $\Pi_{em}^R(Q^2) \equiv \Pi_{em}(Q^2) - \Pi_{em}(0)$, and $f(Q^2)$ is a weight function which has the following form:

$$f(Q^2) = \frac{m_\mu^2 Q^2 Z^3 (1 - Q^2 Z)}{1 + m_\mu^2 Q^2 Z^2},$$

$$Z \equiv \frac{\sqrt{Q^4 + 4m_\mu^2 Q^2} - Q^2}{2m_\mu^2 Q^2}. \quad (36)$$

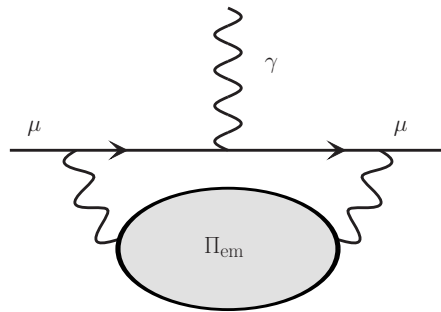


FIG. 1: An illustration of (techni-)HLO contributions to muon $g - 2$.

The formula can be rewritten in terms of Π_V as follows:

$$a_{\mu}^{(\text{techni-})\text{HLO}} = 4\pi^2 \left(\frac{\alpha_{\text{em}}}{\pi} \right)^2 \mathcal{N} \int_0^{\infty} \frac{dQ^2}{Q^2} f(Q^2) (\Pi_V(Q^2) - \Pi_V(0)), \quad (37)$$

where \mathcal{N} is the prefactor in Eq. (33), which takes the following values in the case of QCD and one-family technicolor model [19]:

$$\mathcal{N} \equiv 2 \sum_f q_f^2 = \begin{cases} 10/9 & \text{QCD } (N_f = 2) \\ 4/3 & \text{QCD } (N_f = 3) \\ 16/3 & \text{one-family technicolor} \end{cases} \quad (38)$$

Now, all the physical quantities we are interested in have been expressed in terms of calculable holographic quantities. In the following two sections, for the case of QCD and WTC respectively, we evaluate those physical quantities as functions of the model parameters ξ, z_m, G and γ_m , especially focusing on their dependence on G closely related to the gluon condensate.

III. GLUONIC EFFECTS IN QCD

In this section, we apply the holographic calculations explained in the previous section for the estimation of various physical quantities in the real-life QCD. For this purpose, we take $\gamma_m = 0$ so that the model correctly reproduces the UV asymptotic behavior of the QCD. After fixing the value of γ_m , all the physical quantities are expressed as functions of z_m, ξ and G . We use $M_{\rho} = 775.49$ MeV and $f_{\pi} = 92.4$ MeV as inputs to fix two of these remaining model parameters. Then, from Eqs. (29) and (31), one can express z_m and ξ as functions of G . Now, the remaining physical quantities, namely $M_{a_1}, \langle \frac{\alpha_s}{\pi} G_{\mu\nu}^2 \rangle, (-\langle \bar{q}q \rangle)^{1/3}, M_S, M_G$ and $S = -16\pi L_{10}$ can be expressed as functions of a single parameter G through Eqs. (30), (13), (14), (15), (16) and (32), which are depicted in Fig. 2 by varying G from 0 to 0.4: Observed values of those quantities are also indicated in the plots: two dashed red lines correspond to upper and lower values of 1- σ error band. The ‘‘observed’’ glueball mass M_G has been taken from an expected mass range in lattice simulations [23]. As for the flavor-singlet two-quark bound state S meson, we have chosen $f_0(1370)$ and estimated the ‘‘observed’’ mass neglecting mixing with four-quark bound state $f_0(980)$. (For more detailed discussions, see Ref. [5].)

The figures tell us that the a_1 meson mass M_{a_1} and gluon condensate $\langle \frac{\alpha_s}{\pi} G_{\mu\nu}^2 \rangle$ highly depend on the change of G , while other quantities are rather insensitive to it, keeping values at around observed values of each quantity. From these results, we see the optimal value of G (and hence z_m and ξ): [5]

$$G \simeq 0.25, \quad z_m^{-1} \simeq 347 \text{ MeV}, \quad \xi \simeq 3.1, \quad (39)$$

for the holographic model with $\gamma_m = 0$ to reproduce the QCD observables. In Table I we show the results of holographic calculations for $G = 0.25$ (and $G = 0$ for comparison) along with observed value of each quantity.

We see that the agreement between holographic predictions and the observed values are much improved compared with the case $G = 0$. As was discussed in Ref. [5], nonzero gluonic effects with $G \simeq 0.25$ are important to achieve such a simultaneous agreement of various QCD observables, most notably $\langle \frac{\alpha_s}{\pi} G_{\mu\nu}^2 \rangle$ and M_{a_1} .

Now we discuss the QCD gluonic effect on the hadronic leading order contribution to muon $g - 2$, a_{μ}^{HLO} , which can be calculated through Eq.(37). As was done for calculations of other observables, we take $\gamma_m = 0$, $f_{\pi} = 92.4$ MeV and $M_{\rho} = 775.49$ MeV as inputs, then calculate the value of a_{μ}^{HLO} as a function of G to see gluonic effects on it.

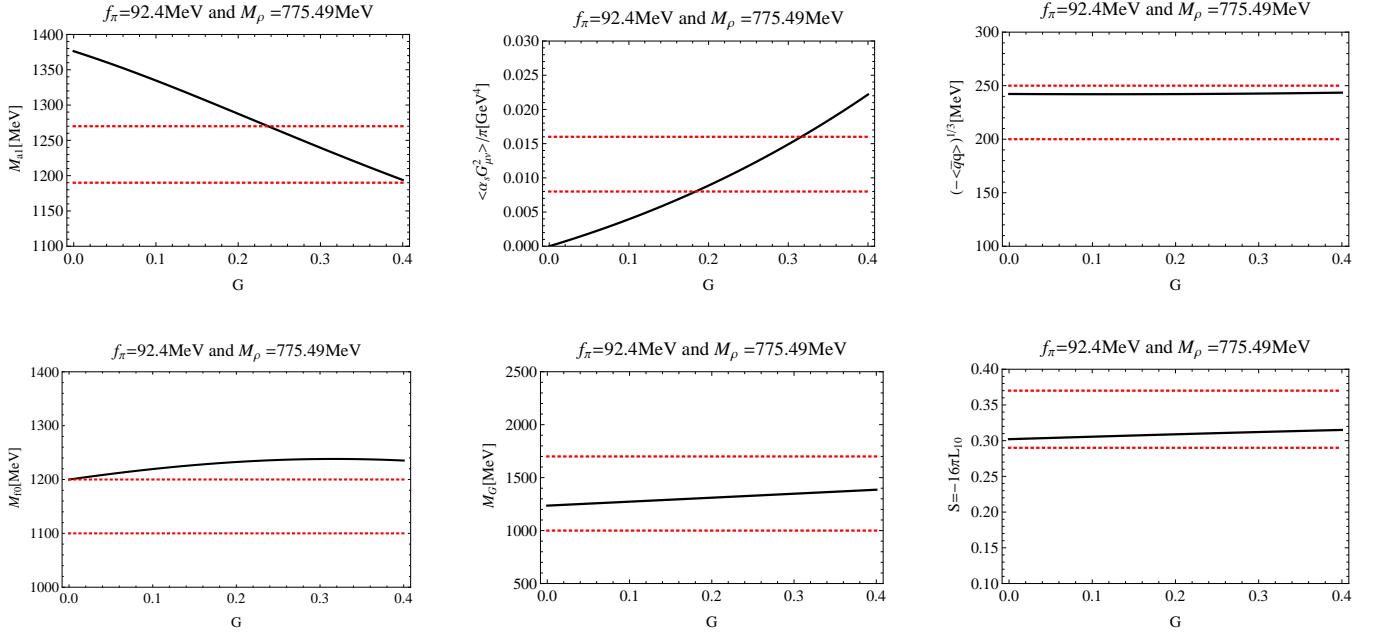


FIG. 2: Plots of various QCD quantities as functions of G with $f_\pi = 92.4$ MeV and $M_\rho = 775.49$ MeV fixed. Top-left: M_{a_1} [20]; Top-center: $\langle \frac{\alpha_s}{\pi} G_{\mu\nu}^2 \rangle$ [21]; Top-right: $(-\langle \bar{q}q \rangle)^{1/3}$ [22]; Bottom-left: $M_{S=f_0(1370)}$ [5]; Bottom-center: M_G [23]; Bottom-right: $S = -16\pi L_{10}$ [24]. Two dashed red lines in each plot correspond to observed upper and lower values of $1\text{-}\sigma$ error band quoted in the corresponding references.

	M_{a_1} [MeV]	$\langle \frac{\alpha_s}{\pi} G_{\mu\nu}^2 \rangle$ [GeV ⁴]	$(-\langle \bar{q}q \rangle)^{1/3}$ [MeV]	$M_{S=f_0(1370)}$ [GeV]	M_G [GeV]	$S = -16\pi L_{10}$
model ($G = 0$)	1376	0	277	1.20	1.24	0.30
model ($G = 0.25$)	1264	0.012	277	1.23	1.33	0.31
measured	1230 ± 40 [20]	0.012 ± 0.004 [21]	225 ± 25 [22]	$1.1 - 1.2$ [5]	$1.0 - 1.7$ [23]	0.33 ± 0.04 [24]

TABLE I: The predicted values of various QCD observables obtained from holographic calculations for $G = 0.25$ (and $G = 0$) with $f_\pi = 92.4$ MeV, $M_\rho = 775.49$ MeV fixed, in comparison with the observed values.

The left panel of Fig. 3 shows the integrand in Eq.(37) as a function of Q^2 varying G from 0 to 0.4 with $f_\pi = 92.4$ MeV and $M_\rho = 775.49$ MeV fixed. We see that as G increases from 0 to 0.4, the peak value at around $Q^2 = m_\mu^2$ becomes larger, leading to the enhancement of a_μ^{HLO} . In the right panel of Fig. 3 we plot a_μ^{HLO} as a function of G for the case of $N_f = 2$ with $f_\pi = 92.4$ MeV and $M_\rho = 775.49$ MeV fixed. As was expected from the enhancement of the integrand, the figure shows that the size of a_μ^{HLO} becomes larger as G increases. The values a_μ^{HLO} at the optimal point ($G = 0.25$) is estimated (in the chiral limit $m_u = m_d = m_s = 0$) as

$$\begin{aligned} a_\mu^{\text{HLO}}|_{N_f=2} &\simeq 505 \times 10^{-10} & \text{at } G = 0.25, \\ a_\mu^{\text{HLO}}|_{N_f=3} &\simeq 606 \times 10^{-10} & \text{at } G = 0.25. \end{aligned} \quad (40)$$

The predicted value for $N_f = 2$ above is in excellent agreement with a partial hadronic contribution to a_μ^{HLO} estimated only from $\sigma(e^+e^- \rightarrow \pi^+\pi^-)$, $a_\mu^{\text{HLO}}|_{\pi^+\pi^-} = (504.2 \pm 3.0) \times 10^{-10}$ [15]. The size of $a_\mu^{\text{HLO}}|_{N_f=3}$ is compared with the full hadronic contributions, $a_\mu^{\text{HLO}}|_{\text{full}} = (694.9 \pm 4.3) \times 10^{-10}$ [15]. Agreements are quite impressive, considering that our estimate is only at chiral limit $m_u = m_d = m_s = 0$.

The above results can be compared to the value of a_μ^{HLO} obtained without gluon condensation effect [14], which can be realized by setting $G = 0$:

$$\begin{aligned} a_\mu^{\text{HLO}}|_{N_f=2} &\simeq 476 \times 10^{-10} & \text{at } G = 0, \\ a_\mu^{\text{HLO}}|_{N_f=3} &\simeq 571 \times 10^{-10} & \text{at } G = 0. \end{aligned} \quad (41)$$

We see that the inclusion of gluonic effect results in enhancement of the value of a_μ^{HLO} by about 6%, and in both

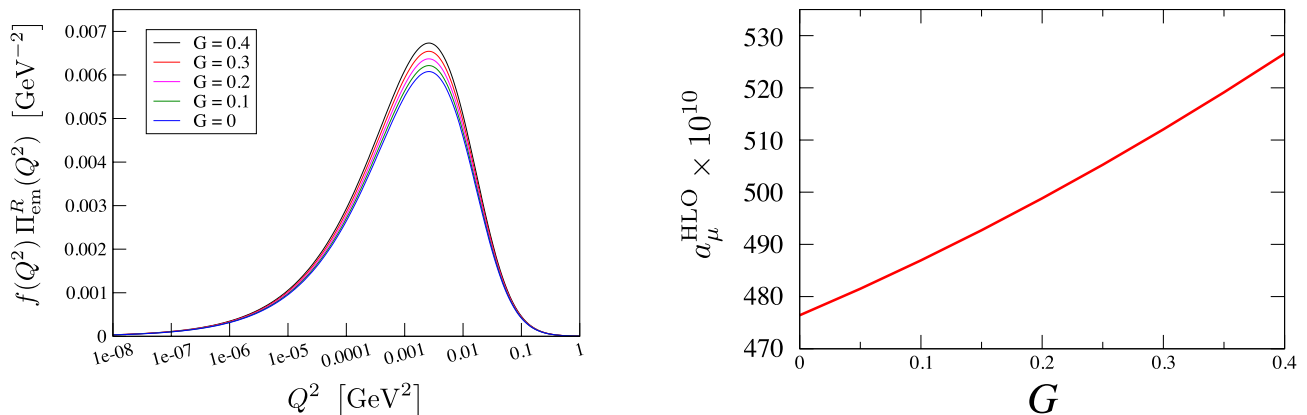


FIG. 3: Left panel: The integrand in Eq.(37) as a function of Q^2 varying G from 0 to 0.4 with $f_\pi = 92.4$ MeV and $M_\rho = 775.49$ MeV fixed. Right panel: a_μ^{HLO} as a function of G for $N_f = 2$ with $f_\pi = 92.4$ MeV and $M_\rho = 775.49$ MeV fixed.

$N_f = 2$ and 3 cases, the agreement between holographic prediction and experimental value becomes better at $G = 0.25$ compared to the results obtained from holographic model without gluonic effect.

Before closing this section, we show the results of similar holographic calculations for the HLO contribution to the anomalous magnetic moment of the electron and the tau lepton. The formulae for a_e^{HLO} and a_τ^{HLO} can be obtained simply by replacing m_μ in Eq. (36) by m_e and m_τ , respectively. In Table II, we show the results in the case of $N_f = 2, 3$ and $G = 0, 0.25$. The values for a_μ^{HLO} are also listed as well. The resultant value of a_e^{HLO} can be compared

	$a_e^{\text{HLO}} \times 10^{14}$	$a_\mu^{\text{HLO}} \times 10^{10}$	$a_\tau^{\text{HLO}} \times 10^8$
$N_f=2, G=0$	125	476	230
$N_f=2, G=0.25$	133	505	239
$N_f=3, G=0$	150	571	276
$N_f=3, G=0.25$	160	606	287

TABLE II: Summary of holographic calculations for the HLO contribution to the anomalous magnetic moment of leptons. $f_\pi=92.4$ MeV and $M_\rho=775.4$ MeV are used as inputs.

to the value $\sim 186.6(\pm 1.1) \times 10^{-14}$, which was obtained in Ref. [25] by using the same $e^+e^- \rightarrow$ hadrons data as those used in Ref. [15]. As for a_τ^{HLO} , it is roughly $(200 - 400) \times 10^{-8}$. (See, for example, Table 1 in Ref. [26] for a nice summary of various estimations of a_τ^{HLO} .) It is remarkable that the holographic predictions of the HLO contribution to $g - 2$ are quite consistent with the known values for all leptons. Considering the fact that the energy scales which are important for determining a_e^{HLO} , a_μ^{HLO} and a_τ^{HLO} are $Q^2 \sim m_e^2, m_\mu^2$ and m_τ^2 respectively, the above mentioned good agreement indicates that the holographic calculation of $\Pi_{\text{em}}(Q^2)$ is quite reliable in a *wide range of the continuous space-like momentum*, not just in the range of the (discrete) time-like momentum where the resonance parameters are fitted in the conventional holographic studies in the zero-width approximation (large N_c limit).

IV. GLUONIC EFFECTS IN WALKING TECHNICOLOR

If the EW symmetry is dynamically broken by WTC, it is natural to expect that there are techni-hadronic contributions to the anomalous magnetic moment of leptons in a way analogous to the QCD HLO contributions. In this section, we estimate such effects in WTC. Throughout calculations in this section, we take $\gamma_m = 1$ for the bulk scalar mass term, instead of $\gamma_m = 0$ for QCD in the previous section, so that the model reproduces desired walking behavior of WTC. To be concrete, we take the one-family model[19] for the WTC as an example, in which case the number of techni-fermion is $N_f = 8$, having $N_D = 4$ weak doublet in the model. Actually, recent lattice results for $SU(3)$ gauge theories suggest that $N_f = 8$ is a walking theory [27]. The techni-pion decay constant F_π is related to the EW scale v_{EW} as $F_\pi = v_{\text{EW}}/\sqrt{N_D}$, therefore, in the case of one-family WTC model, it is fixed to be $F_\pi = 246\text{GeV}/\sqrt{4} = 123$

GeV. In order to see the dependence of physical observables on G in WTC, we further fix the holographic infrared scale z_m^{-1} at typical values $z_m^{-1} = 2, 4, 6$ TeV, which roughly covers the phenomenologically interesting region of the S parameter [16], $0.1 < S < 1.0$. (see discussions below).

In Fig. 4 we show the G dependences of various observables in the case of $N_{\text{TC}} = 3$: the TD mass M_ϕ (Top-left), the S parameter (Top-center), the masses of techni- ρ (M_ρ) and techni- a_1 (M_{a_1}), degenerate each other (Top-right), the chiral condensate $\langle \bar{F}F \rangle$ (Bottom-left), the gluon condensate $\langle \frac{\alpha}{\pi} G_{\mu\nu}^2 \rangle$ (Bottom-center), and the techni-glueball mass M_G (Bottom-right). Remarkably enough, the TD mass M_ϕ (top-right figure) dramatically changes from the order of

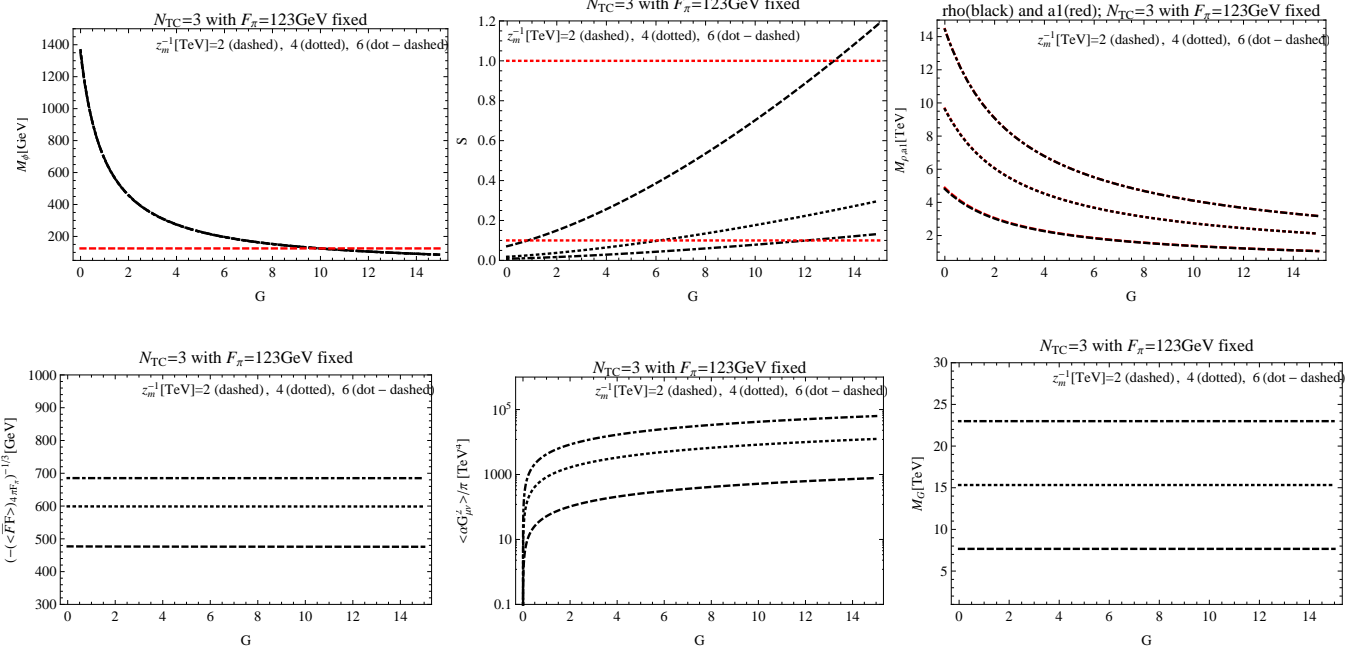


FIG. 4: Various quantities as functions of G for the one-family WTC with $N_{\text{TC}} = 3$ and $F_\pi = 123$ GeV fixed. Here, we have taken $z_m^{-1} = 2$ (dashed curve), 4 (dotted curve) and 6 (dot-dashed curve) TeV. Top-left: M_ϕ (Since three curves lie on top of one another, they are almost indistinguishable in the figure. The red dotted line indicates $M_\phi = 125$ GeV), Top-center: S parameter (The red dotted line indicates $S = 0.1$), Top-right: M_ρ (black curves) and M_{a_1} (red curves) (Note that ρ and a_1 are almost degenerate), Bottom-left: $(-\langle \bar{F}F \rangle_{\mu=4\pi F_\pi})^{1/3}$, Bottom-center: $\langle \frac{\alpha}{\pi} G_{\mu\nu}^2 \rangle$, Bottom-right: M_G .

TeV down to 100 GeV as G varies from 0 to $G = O(10)$ [5, 6]. Actually, we can obtain a sensible vanishing TD mass limit, *quite independently* of z_m^{-1} [6]:

$$\frac{M_\phi}{4\pi F_\pi} \simeq \sqrt{\frac{3}{N_{\text{TC}}}} \frac{\sqrt{3}/2}{1+G} \rightarrow 0 \quad (G \rightarrow \infty). \quad (42)$$

Thus in order to have a naturally light TD in the WTC case, we need the role of the gluon condensate more eminent than in QCD. Since we identify the TD, flavor-singlet scalar ϕ , as the 125 GeV boson discovered at the LHC [9] #3, we refer to the value of G which reproduces $M_\phi \simeq 125$ GeV as the “physical point”. In the top-left panel of Fig. 4, we indicated $M_\phi = 125$ GeV as red-dashed line, so that we can easily find the physical point. From the figure, in the case of $N_{\text{TC}} = 3$, one can see that the value of $G \simeq 10$ at the physical point is rather insensitive to the values of z_m^{-1} .

As to the S parameter, it increases as G grows. However, we can see from Fig. 4 that we can *freely adjust a small S parameter*, say $S < 0.1$, by increasing z_m^{-1} (or equivalently increasing M_ρ), *without affecting the LHC phenomenology* of the physical point $M_\phi = 125$ GeV (and also couplings) which is quite independent of z_m^{-1} [6]. Here we are particularly interested in the region, $0.1 < S < 1.0$, corresponding to the lighter M_{ρ/a_1} accessible at the future LHC. Note that $S \propto F_\pi^2/M_\rho^2$ [5, 6]. Although $S = 0.1$ is a phenomenologically viable benchmark value, there is a possibility that even if the WTC dynamics itself produces a large value of S , contributions coming from other part of the model such as

#3 As was shown in Refs. [6, 13], the TD in the one-family WTC indeed has the LHC signal consistent with the currently reported experimental data, notably explains the diphoton excess [9].

the ETC interactions could partially cancel it in a way similar to the concept of fermion-delocalization effect studied in Higgsless models [28]. (In this sense $S > 1.0$ might also be viable and even more interesting in view of having much lighter M_{ρ/a_1} below TeV to be tested at the LHC.)

In accord with $S \propto F_\pi^2/M_\rho^2$, we see in the Top-right figure in Fig. 4 that M_ρ and M_{a_1} substantially decrease as the value of G increases, which would imply that the masses M_ρ and M_{a_1} at $G = 0$ solely generated by the chiral condensate are drastically reduced by the large gluonic contributions. Also note the almost degenerate masses for all G getting eventually degenerate at large G [5, 6]. See Fig.5. It is also noted that this degeneracy does not imply a big cancellation of both contributions so as to yield a small S parameter.

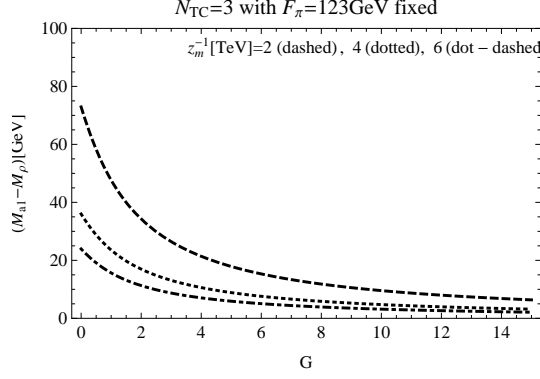


FIG. 5: G dependence of the degeneracy of the mass of techni- ρ and techni- a_1 for $N_{\text{TC}} = 3$ at $F_\pi = 123$ GeV and $z_m^{-1} = 2, 4, 6$ TeV.

We can also do similar calculations for the case of $N_{\text{TC}} = 4$ and 5. The holographic parameters (G, z_m^{-1}, ξ) at the physical points $M_\phi = 125$ GeV for $S = (0.1, 0.3, 1.0)$ in the cases of $N_{\text{TC}} = 3, 4$ and 5 are summarized as [6]:

$$\begin{aligned} G \simeq 10, z_m^{-1}[\text{TeV}] &= (5.3, 3.1, 1.7), \xi = (0.01, 0.02, 0.04) & \text{for } N_{\text{TC}} = 3, \\ G \simeq 8.5, z_m^{-1}[\text{TeV}] &= (4.8, 2.8, 1.5), \xi = (0.01, 0.03, 0.05) & \text{for } N_{\text{TC}} = 4, \\ G \simeq 7.5, z_m^{-1}[\text{TeV}] &= (4.5, 2.6, 1.4), \xi = (0.02, 0.03, 0.05) & \text{for } N_{\text{TC}} = 5, \end{aligned} \quad (43)$$

which is compared with Eq.(39) in QCD. In Table III we make a list of the predicted values of various quantities at the physical point for the cases of $N_{\text{TC}} = 3, 4$ and 5 for the phenomenologically interesting values $S = (0.1, 0.3, 1.0)$.

N_{TC}	G	M_ϕ [GeV]	M_ρ [TeV]	M_{a_1} [TeV]	M_G [TeV]	$(-\langle \bar{F}F \rangle_{\mu=4\pi F_\pi})^{1/3}$ [GeV]	$\frac{1}{\pi} \langle \alpha G_{\mu\nu}^2 \rangle$ [TeV ⁴]
3	10	(124, 125, 125)	(3.6, 2.1, 1.1)	(3.6, 2.1, 1.2)	(20, 11, 5.4)	(658, 530, 423)	(2.6, 0.16, 0.0094) $\times 10^4$
4	8.5	(125, 125, 126)	(3.6, 2.1, 1.1)	(3.6, 2.1, 1.2)	(20, 11, 5.4)	(628, 505, 405)	(2.6, 0.16, 0.0095) $\times 10^4$
5	7.5	(125, 125, 126)	(3.6, 2.1, 1.1)	(3.6, 2.1, 1.2)	(20, 11, 5.4)	(604, 486, 388)	(2.6, 0.16, 0.0095) $\times 10^4$

TABLE III: The predicted values of various observables in WTC with $N_{\text{TC}} = 3, 4, 5$ at the physical point shown in Eq.(43) and $F_\pi = 123$ GeV. Three values in each parenthesis in the table correspond to the cases of $S = (0.1, 0.3, 1.0)$ from left to right, respectively.

It should be noted that the value of G at the physical point is quite large in the case of WTC compared to the case of QCD, whose physical point is $G = 0.25$ (see Table I and discussion around Eq. (39)). Thus the inclusion of the gluonic effects plays a vital role for the holographic calculations of physical quantities in the case of WTC. This is also the case for the techni-HLO contributions to the anomalous magnetic moment of leptons as we will see below.

Let us now evaluate the gluonic effect on the techni-HLO contributions to the muon $g - 2$. In Fig. 6, we plot the results of holographic calculations of the techni-HLO contribution to the anomalous magnetic moment of the muon, $a_\mu^{\text{techni-HLO}}$, as a function of G in the case of the one-family WTC for $N_{\text{TC}} = 3$ (solid curve), 4 (dashed curve) and 5 (dotted curve) with $F_\pi = 123$ GeV, $M_\phi = 125$ GeV and $z_m^{-1} = 2$ (black), 4 (red), 6 (blue) TeV. From this figure, we see a general trend that the value of $a_\mu^{\text{techni-HLO}}$ monotonically increases as a function of G for all the combinations of N_{TC} and z_m^{-1} : The physical point $G \simeq 10$ ($M_\phi = 125$ GeV) implies about 10^2 times enhancement compared with the $G = 0$ value.

In Table IV, we list explicit values of $a_\mu^{\text{techni-HLO}}$ at $G = 0$ and those at the physical point for each combination of N_{TC} under the phenomenological constraint on the S parameter (see Fig. 4 (Top-center panel) for G -dependence

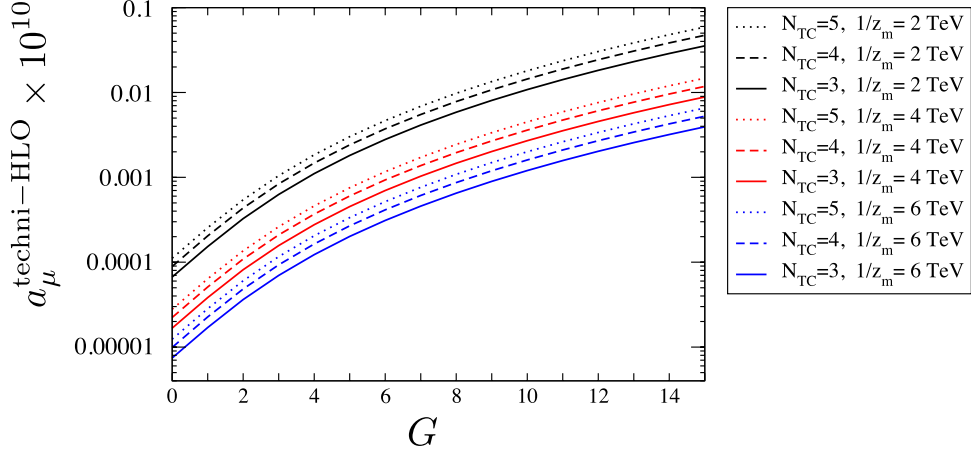


FIG. 6: $a_\mu^{\text{techni-HLO}}$ as a function of G in the case of the one-family WTC for $N_{\text{TC}} = 3$ (solid), 4 (dashed) and 5 (dotted) with $F_\pi = 123$ GeV, $M_\phi = 125$ GeV and $z_m^{-1} = 2$ TeV (black), 4 TeV (red), and 6 TeV (blue) fixed.

of S), so that we can easily see how much the value of $a_\mu^{\text{techni-HLO}}$ at the physical point is enhanced by the gluon-condensation effect under such a constraint. From this table, we see that, in most cases, the value of $a_\mu^{\text{techni-HLO}}$ at

$N_{\text{TC}} = 3$	$a_\mu^{\text{techni-HLO}} \times 10^{10}$	$N_{\text{TC}} = 4$	$a_\mu^{\text{techni-HLO}} \times 10^{10}$	$N_{\text{TC}} = 5$	$a_\mu^{\text{techni-HLO}} \times 10^{10}$
$S = 0.1, G = 0$	0.0000946	$S = 0.1, G = 0$	0.000125	$S = 0.1, G = 0$	0.000156
$S = 0.1, G = 10$	0.00153	$S = 0.1, G = 8.5$	0.00159	$S = 0.1, G = 7.5$	0.00164
$S = 0.3, G = 0$	0.000298	$S = 0.3, G = 0$	0.000390	$S = 0.3, G = 0$	0.000482
$S = 0.3, G = 10$	0.00460	$S = 0.3, G = 8.5$	0.00477	$S = 0.3, G = 7.5$	0.00494
$S = 1.0, G = 0$	0.00126	$S = 1.0, G = 0$	0.00152	$S = 1.0, G = 0$	0.00180
$S = 1.0, G = 10$	0.0155	$S = 1.0, G = 8.5$	0.0160	$S = 1.0, G = 7.5$	0.0166

TABLE IV: Comparison of values of $a_\mu^{\text{techni-HLO}}$ of the one-family WTC at $G = 0$ and at the physical point for each combination of N_{TC} and S . Here, F_π and M_ϕ are fixed to be $F_\pi = 123$ GeV and $M_\phi = 125$ GeV, respectively.

the physical point is more than 10 times larger than the value at $G = 0$ for $S = 0.1$. Also, for any given combination of N_{TC} and G , the value of $a_\mu^{\text{techni-HLO}}$ is enhanced by another factor of more than 10 when we change the constraint on S from 0.1 to 1.0. (If we are allowed to take even larger S such as $S > 1.0$ for the reason we mentioned before, we would get further drastically large enhancement.)

These trends are visibly understood from Fig. 7, where we plotted contributions to $\Pi_{\text{em}}^R(Q^2)$ from QCD, as well as that from WTC dynamics in comparison between $(G, S) = (10, 0.1)$ and $(0, 0.1)$ to show the enhancement of $a_\mu^{\text{techni-HLO}}$ simply due to the increased gluonic effects G for the same S value. We also included the data for $(G, S) = (10, 1.0), (10, 0.3)$ just for illustration of this enhancement by the change from $G = 0$ to $G = 10$ could be amplified if we relax the S parameter constraint. In the figure, we also plotted weight function in Eq. (36) for the muon (denoted as $f_\mu(Q^2)$ in the figure) in unit of GeV^{-2} . The energy scale at which the slope (in the log-log plot) of the weight function changes roughly corresponds to the scale where the integrand in Eq. (35) has its peak, namely $Q^2 \sim m_\mu^2 \simeq 0.01 \text{ GeV}^2$. Therefore, very roughly speaking, the contribution to $a_\mu^{\text{techni-HLO}}$ is proportional to the magnitude of $\Pi_{\text{em}}^R(Q^2)$ at this scale. It should be noted that $\Pi_{\text{em}}^R(Q^2)|_{\text{QCD}}/\Pi_{\text{em}}^R(Q^2)|_{\text{WTC}}$ is almost constant at around $Q^2 \sim m_\mu^2 \simeq 0.01 \text{ GeV}^2$, while the ratio becomes larger at $Q^2 \sim m_\tau^2 \simeq 3 \text{ GeV}^2$. This implies that the WTC contribution gets relatively more important in the case of tau $g-2$. In Table V, we summarize the size of contributions to $a_\mu^{\text{techni-HLO}}$ and $a_\tau^{\text{techni-HLO}}$ from QCD and WTC at the physical point. As for WTC contributions, two cases (i.e., $S = 0.1$ and 1.0) are shown in the table. As we expect, $a_\tau^{\text{HLO}}/a_\tau^{\text{techni-HLO}}$ is about 6 times larger compared to the ratio in the case of muon $g-2$.

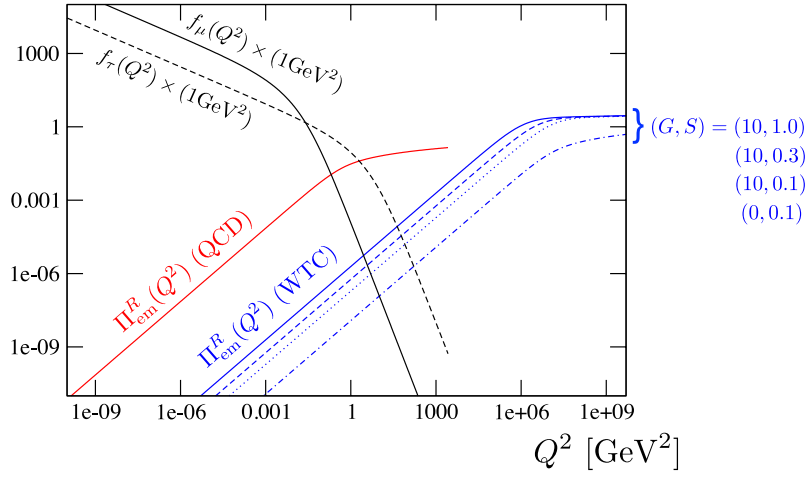


FIG. 7: Black solid (dashed) curve represents weight function $f(Q^2)$ in Eq. (36) for the muon (tau lepton) in unit of GeV^{-2} . Red solid curve represents renormalized electromagnetic current correlator $\Pi_{\text{em}}^R(Q^2)$ which comes from vacuum polarization due to QCD. Blue curves are contributions to $\Pi_{\text{em}}^R(Q^2)$ from WTC dynamics with $N_{TC} = 3$ and $F_\pi = 123$ GeV fixed: Dotted and dashed-dotted curves correspond to the cases of $(G, S) = (10, 0.1)$ and $(0, 0.1)$, respectively. This enhancement due to $G = 0 \rightarrow 10$ is more eminent as illustrated by the solid and dashed-dotted curves, $(G, S) = (10, 1.0)$, $(10, 0.3)$, respectively.

	$a_\mu^{(\text{techni-})\text{HLO}} \times 10^{10}$	$a_\tau^{(\text{techni-})\text{HLO}} \times 10^8$
QCD ($N_f = 3$) : $f_\pi = 92.4$ MeV, $M_\rho = 775.49$ MeV, $G = 0.25$	606	287
WTC ($N_{TC} = 3$) : $F_\pi = 123$ GeV, $S = 0.1$, $G = 10$	0.00153	0.00433
WTC ($N_{TC} = 3$) : $F_\pi = 123$ GeV, $S = 1.0$, $G = 10$	0.0155	0.0437

TABLE V: Summary of holographic calculations of contributions to $a_\mu^{(\text{techni-})\text{HLO}}$ and $a_\tau^{(\text{techni-})\text{HLO}}$ from QCD and WTC dynamics at the physical point. Two cases, $S = 0.1$ and 1.0 , are shown for WTC contribution.

V. DISCUSSION AND CONCLUSIONS

We have shown the results of holographic calculations of the (techni-)HLO contributions to the anomalous magnetic moment $g - 2$ of leptons. It was shown that, in the case of the QCD contribution, it was enhanced by about 6% due to the proper inclusion of the gluon-condensation effect ($G = 0.25$) compared to the estimate ignoring it ($G = 0$) [14], leading to a better agreement with the known value determined by the experimental data [15]:

$$a_\mu^{\text{HLO}}|_{N_f=2} \simeq 505 \times 10^{-10} \quad (a_\mu^{\text{HLO}}|_{\pi^+\pi^-} = (504.2 \pm 3.0) \times 10^{-10}), \quad (44)$$

$$a_\mu^{\text{HLO}}|_{N_f=3} \simeq 606 \times 10^{-10} \quad (a_\mu^{\text{HLO}}|_{\text{full}} = (694.9 \pm 4.3) \times 10^{-10}). \quad (45)$$

Considering that our estimate was at the chiral limit ($m_u = m_d = m_s = 0$), the agreement is rather impressive.

In the case of WTC, where the gluonic effect plays more significant role compared to the case of QCD to reproduce the observed 125 GeV scalar boson, the gluon-condensation effects are more dramatic for the muon $g - 2$: The value of the techni-HLO contribution at physical value $G \simeq 10$ is more than 100 times larger compared to the estimate ignoring the gluonic effect ($G = 0$), if we allow rather large value of S up to $S < 1.0$.

It is quite interesting that the contributions to the anomalous magnetic moment from the vacuum polarization of the electromagnetic current is several orders of magnitude larger than the naive scale-up estimate, which is obtained by simply multiplying the ratio of the squares of typical scales of QCD ($f_\pi \simeq 92$ MeV) to one-family model ($F_\pi \simeq 123$ GeV) to the value of a_μ^{HLO} , yielding a value of $\simeq 3 \times 10^{-14}$. This value roughly coincides with the value of holographic calculation with $G = 0$, $S = 0.3$ (see Table IV).

Though this kind of significant enhancement is quite interesting theoretically, the phenomenological interest is whether WTC contribution is visible or not. Even if there is an enhancement by several orders of magnitudes compared to the naive estimate, the contribution from the WTC dynamics to the $g - 2$ is still negligibly small

compared to the QCD contribution. The magnitude of WTC contribution to the muon $g - 2$ is, at most, order of 10^{-12} for the cases of setup investigated in this paper. This value is still quite small compared to the current discrepancy between the experimental value of the muon $g - 2$ and the standard model prediction of it: $\delta a_\mu \equiv a_\mu^{\text{Exp}} - a_\mu^{\text{SM}} = (26.1 \pm 8.0) \times 10^{-10}$ [15, 29]. Therefore, it seems rather unlikely that the contributions from WTC dynamics can explain the current 3.3σ deviation between experiment and the SM prediction.

In conclusion we have shown, in a bottom-up holographic model for QCD/WTC, that the amount of gluonic effects to realize the physical point ($G = 0.25$ for QCD and $G = 10$ for WTC with $N_{\text{TC}} = 3$) makes significant effects enhancing the (techni-) HLO contributions to the lepton $g - 2$. Since the introduction of the gluonic effects in this model is just to make the model consistent with the high energy region of the QCD, it is a highly nontrivial test of this holographic model whether or not the effects also improve the agreements with the low energy hadron physics, particularly in the most relevant momentum region $Q^2 = -q^2 \sim m_l^2$ for ($l = e, \mu, \tau$) (see Fig.7), which is far infrared region for QCD. Note that the quantity studied in this paper is in the space-like momentum region $Q^2 > 0$ which is theoretically more tractable without limitation of the zero-width constraint of large N_c limit where the holography is so far justified, in contrast to the resonance phenomenology in the time-like region. Our work presents an explicit example of a holographic model which successfully reproduces the QCD physics in all energy region from the very ultraviolet region for OPE all the way down to such a deep infrared region in the space-like momentum. The vital role of the gluon condensate in WTC in connection with the light scalar composite can be clarified by the future lattice studies such as an extension of the work which observed a light flavor-singlet scalar meson in large N_f QCD [30].

Acknowledgments

This work was supported by the JSPS Grant-in-Aid for Scientific Research (S) #22224003 and (C) #23540300 (K.Y.).

-
- [1] J. M. Maldacena, *Adv. Theor. Math. Phys.* **2**, 231 (1998) [*Int. J. Theor. Phys.* **38**, 1113 (1999)].
 - [2] L. Da Rold and A. Pomarol, *Nucl. Phys. B* **721**, 79 (2005).
 - [3] J. Erlich, E. Katz, D. T. Son and M. A. Stephanov, *Phys. Rev. Lett.* **95**, 261602 (2005).
 - [4] T. Sakai and S. Sugimoto, *Prog. Theor. Phys.* **113**, 843 (2005).
 - [5] K. Haba, S. Matsuzaki and K. Yamawaki, *Phys. Rev. D* **82**, 055007 (2010).
 - [6] S. Matsuzaki and K. Yamawaki, *Phys. Rev. D* **86**, 115004 (2012).
 - [7] K. Yamawaki, M. Bando and K. Matumoto, *Phys. Rev. Lett.* **56**, 1335 (1986); M. Bando, T. Morozumi, H. So and K. Yamawaki, *Phys. Rev. Lett.* **59**, 389 (1987).
 - [8] M. Bando, K. Matumoto and K. Yamawaki, *Phys. Lett. B* **178**, 308 (1986).
 - [9] S. Chatrchyan *et al.* [CMS Collaboration], *Phys. Lett. B* **716**, 30 (2012); G. Aad *et al.* [ATLAS Collaboration], *Phys. Lett. B* **716**, 1 (2012).
 - [10] M. Harada, M. Kurachi and K. Yamawaki, *Phys. Rev. D* **68**, 076001 (2003); M. Kurachi and R. Shrock, *JHEP* **0612**, 034 (2006).
 - [11] S. Shuto, M. Tanabashi and K. Yamawaki, in *Proc. 1989 Workshop on Dynamical Symmetry Breaking*, Dec. 21-23, 1989, Nagoya, eds. T. Muta and K. Yamawaki (Nagoya Univ., Nagoya, 1990) 115-123; M. S. Carena and C. E. M. Wagner, *Phys. Lett. B* **285**, 277 (1992); M. Hashimoto, *Phys. Lett. B* **441**, 389 (1998).
 - [12] M. Hashimoto and K. Yamawaki, *Phys. Rev. D* **83**, 015008 (2011).
 - [13] S. Matsuzaki and K. Yamawaki, *Phys. Rev. D* **85**, 095020 (2012); *Phys. Rev. D* **86**, 035025 (2012); *Phys. Lett. B* **719**, 378 (2013).
 - [14] D. K. Hong, D. Kim and S. Matsuzaki, *Phys. Rev. D* **81**, 073005 (2010).
 - [15] K. Hagiwara, R. Liao, A. D. Martin, D. Nomura and T. Teubner, *J. Phys. G* **38**, 085003 (2011).
 - [16] M. E. Peskin and T. Takeuchi, *Phys. Rev. Lett.* **65** (1990), 964; *Phys. Rev. D* **46** (1992), 381; B. Holdom and J. Terning, *Phys. Lett. B* **247** (1990), 88; M. Golden and L. Randall, *Nucl. Phys. B* **361** (1991), 3.
 - [17] K. Haba, S. Matsuzaki and K. Yamawaki, *Prog. Theor. Phys.* **120**, 691 (2008).
 - [18] T. Blum, *Phys. Rev. Lett.* **91**, 052001 (2003); C. Aubin and T. Blum, *Phys. Rev. D* **75**, 114502 (2007).
 - [19] E. Farhi and L. Susskind, *Phys. Rev. D* **20**, 3404 (1979).
 - [20] J. Beringer *et al.* [Particle Data Group Collaboration], *Phys. Rev. D* **86**, 010001 (2012).
 - [21] M. A. Shifman, A. I. Vainshtein and V. I. Zakharov, *Nucl. Phys. B* **147**, 385 (1979); *Nucl. Phys. B* **147**, 448 (1979).
 - [22] J. Gasser and H. Leutwyler, *Phys. Rept.* **87**, 77 (1982).
 - [23] For a recent review, see W. Ochs, arXiv:1301.5183 [hep-ph].
 - [24] M. Harada and K. Yamawaki, *Phys. Lett. B* **297**, 151 (1992).
 - [25] D. Nomura and T. Teubner, *Nucl. Phys. B* **867**, 236 (2013).
 - [26] S. Eidelman and M. Passera, *Mod. Phys. Lett. A* **22**, 159 (2007).

- [27] Y. Aoki, T. Aoyama, M. Kurachi, T. Maskawa, K.-i. Nagai, H. Ohki, A. Shibata, K. Yamawaki and T. Yamazaki, Phys. Rev. D **78**, 094511 (2013).
- [28] G. Cacciapaglia, C. Csaki, C. Grojean and J. Terning, Phys. Rev. D **71**, 035015 (2005); R. Foadi, S. Gopalakrishna and C. Schmidt, Phys. Lett. B **606**, 157 (2005); R. S. Chivukula, E. H. Simmons, H. J. He, M. Kurachi and M. Tanabashi, Phys. Rev. D **72**, 016008 (2005).
- [29] G. W. Bennett *et al.* [Muon G-2 Collaboration], Phys. Rev. D **73**, 072003 (2006).
- [30] Y. Aoki, T. Aoyama, M. Kurachi, T. Maskawa, K.-i. Nagai, H. Ohki, E. Rinaldi, A. Shibata, K. Yamawaki and T. Yamazaki, arXiv:1305.6006 [hep-lat].